applied sciences

MDPI

Article

Physicochemical Characterization of Hyaluronic Acid and Chitosan Liposome Coatings

Claudia Bonechi [1,2,*], Gabriella Tamasi [1,2], Alessandro Donati [1,2], Gemma Leone [1,3], Marco Consumi [1,3], Lorenzo Cangeloni [1,2], Vanessa Volpi [1,2], Agnese Magnani [1,3,*], Andrea Cappelli [1] and Claudio Rossi [1,2]

1 Department of Biotechnology, Chemistry and Pharmacy, University of Siena, Via Aldo Moro 2, 53100 Siena, Italy; gabriella.tamasi@unisi.it (G.T.); alessandro.donati@unisi.it (A.D.); gemma.leone@unisi.it (G.L.); marco.consumi@unisi.it (M.C.); cangeloni@student.unisi.it (L.C.); vanessa.volpi@unisi.it (V.V.); andrea.cappelli@unisi.it (A.C.); claudio.rossi@unisi.it (C.R.)
2 Centre for Colloid and Surface Science (CSGI), University of Florence, Via della Lastruccia 3, Sesto Fiorentino, 50019 Florence, Italy
3 National Interuniversity Consortium of Materials Science and Technology (INSTM), Via G. Giusti 9, 50121 Florence, Italy
* Correspondence: claudia.bonechi@unisi.it (C.B.); agnese.magnani@unisi.it (A.M.); Tel.: +39-0577-232123 (C.B.); +39-0577-232108 (A.M.)

Abstract: Hyaluronic acid (HA) and chitosan (CH) are biopolymers that are widely used in many biomedical applications and for cosmetic purposes. Their chemical properties are fundamental to them working as drug delivery systems and improving their synergistic effects. In this work, two different protocols were used to obtain zwitterionic liposomes coated with either hyaluronic acid or chitosan. Specifically, the methodologies used to perform vesicle preparation were chosen by taking into account the specific chemical properties of these two polysaccharides. In the case of chitosan, liposomes were first synthesized and then coated, whereas the coating of hyaluronic acid was achieved through lipidic film hydration in an HA aqueous solution. The size and the zeta-potential of the polysaccharide-coated liposomes were determined by dynamic light scattering (DLS). This approach allowed coated liposomes to be obtained with hydrodynamic diameters of 264.4 ± 12.5 and 450.3 ± 16.7 nm for HA- and CH-coated liposomes, respectively. The chemical characterization of the coated liposomal systems was obtained by surface infrared (ATR-FTIR) and nuclear magnetic resonance (NMR) spectroscopies. In particular, the presence of polysaccharides was confirmed by the bands assigned to amides and saccharides being in the 1500–1700 cm^{-1} and 800–1100 cm^{-1} regions, respectively. This approach allowed confirmation of the efficiency of the coating processes, evidencing the presence of HA or CH at the liposomal surface. These data were also supported by time-of-flight secondary ion mass spectrometry (ToF-SIMS), which provided specific assessments of surface (3–5 nm deep) composition and structure of the polysaccharide-coated liposomes. In this work, the synthesis and the physical chemistry characterization of coated liposomes with HA or CH represent an important step in improving the pharmacological properties of drug delivery systems.

Keywords: drug delivery system; liposome coating; hyaluronic acid; chitosan; polymeric materials; nanomaterials

check for updates

Citation: Bonechi, C.; Tamasi, G.; Donati, A.; Leone, G.; Consumi, M.; Cangeloni, L.; Volpi, V.; Magnani, A.; Cappelli, A.; Rossi, C. Physicochemical Characterization of Hyaluronic Acid and Chitosan Liposome Coatings. *Appl. Sci.* **2021**, *11*, 12071. https://doi.org/10.3390/app112412071

Academic Editor: Nagendra Kumar Kaushik

Received: 17 November 2021
Accepted: 15 December 2021
Published: 17 December 2021

Publisher's Note: MDPI stays neutral with regard to jurisdictional claims in published maps and institutional affiliations.

Copyright: © 2021 by the authors. Licensee MDPI, Basel, Switzerland. This article is an open access article distributed under the terms and conditions of the Creative Commons Attribution (CC BY) license (https://creativecommons.org/licenses/by/4.0/).

1. Introduction

Liposomes are self-assembled phospholipid structures showing biocompatibility properties. These systems have been applied to improve the bioavailability of hydrophobic bioactive compounds. Liposomes and nanoparticles are widely used for stabilizing drugs and improving their pharmacological properties by acting as carriers in drug delivery processes and promoting the controlled release of drugs at selected target sites [1]. By modifying the surface of these carriers with polymers, such as polyethylene glycol, they become able to prevent mechanisms of plasma–protein adsorption, interfering with the

recognition by the reticuloendothelial system [2,3]. These vesicles are known as stealth liposomes, and their ability to prolong blood circulation, improving the pharmacological effects of drugs, is well documented [4–6]. On the other hand, these systems provide new opportunities in the field of pharmaceutical research and the design of innovative liposomes. To inhibit/reduce chemical degradation of a liposome and undesirable loss of the encapsulated drug, polymers can be used to modify the physicochemical properties of vesicles [7,8]. In particular, the surface properties can be modified to reduce toxicity and to control drug release [9,10]. Coated liposomes have demonstrated that drug activity was synergically increased, along with many other desirable biological effects [11]. The surface modification of liposomes can be obtained by following different processes, such as polymer adsorption [12]. Furthermore, surface coating with a polymer is able to preserve liposome stability [13], and this behavior depends on the ability of the polymer to adhere to the lipid bilayers [14].

Two different strategies can be considered to modify the liposome surface: (i) the classical adsorption of a polymer, promoting an excess of polymer in solution and inducing a random distribution at the surface and (ii) the innovative hydration of phospholipids from a polymeric solution [15]. Moreover, liposomes are systems that are thermodynamically unstable and the coating could interfere, decreasing the colloidal stability. The study of chemical modification of vesicles becomes a very challenging aspect and highlights potential new target sites and applications [16].

Two different polymers were used in the present study to obtain the surface modification of liposomes: chitosan (CH; molecular weight: 50–190 kDa; Figure 1a) and hyaluronic acid (HA; molecular weight: 8.7 kDa; Figure 1b), both at low molecular weights. Chitosan is a linear copolymer composed of D-glucosamine and N-acetyl-D-glucosamine units, linked via β-(1 → 4) bonds. It is a biodegradable polymer obtained from the alkaline deacetylation of chitin [17].

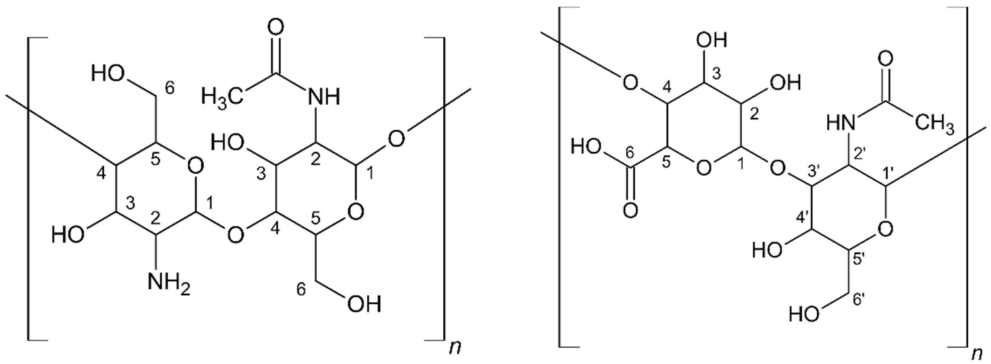

(**a**) (**b**)

Figure 1. Numbering and chemical structure of (**a**) chitosan (CH) and (**b**) hyaluronic acid (HA).

Chitosan is one of the most widely used biopolymers in biomedical applications (textiles, cosmetics and food treatment) due to its ability to bind to a variety of natural or synthetic species such as nanoparticles, polymers, metal ions and cell surfaces. Moreover, owing to its high biocompatibility, biodegradability, absorption capacity and non-antigenicity, chitosan gels and supports are often adopted in the biomedical field and for the synthesis of organic–inorganic nanocomposites with bioactive substrates. Chitosan-coated liposomes have been used as a mucoadhesive delivery system. Their positively charged surface favors adhesion to cell membranes, which are normally negatively charged [14].

Hyaluronic acid is an anionic glycosaminoglycan and is one of the fundamental components of the connective tissue of humans and mammals. HA is a polymer constituted of disaccharides, D-glucuronic acid and N-acetyl-D-glucosamine, connected by alternating β-(1 → 4) and β-(1 → 3) glycosidic bonds. HA has a polymeric structure, having different

molecular weights (5 and 20,000 kDa). The molecular weight greatly influences the viscosity of polysaccharide aqueous solutions.

HA presents a high solubility in aqueous systems and plays a fundamental role in the inflammatory process and other physiological processes. HA shows high biocompatibility and has many uses in the biomedical field [18]. The use of HA as a polymer coating for liposomes is encouraged by its properties of being a protector against vesicle leakage [19], stealth enhancer [20] and lyoprotectant [21].

In this paper, chitosan and hyaluronic acid were used as coatings for DOPC/DOPE zwitterionic liposomes. Liposomes that were coated and purified were characterized through the study of their physical properties, such as the hydrodynamic diameter, ζ-potential and polydispersity index (PDI), which also provide useful information on its stability. Subsequently, the chemical characterization of the coated liposomal systems was performed by nuclear magnetic resonance (NMR), surface infrared (FTIR-ATR) spectroscopy and time-of-flight secondary ion mass spectrometry (ToF-SIMS) analysis to provide fundamental information for understanding and optimizing the coating processes. The final aim of the present study was to synthesize and fully characterize coated liposomes to obtain vesicles with increased chemical properties for new drug delivery systems. In particular, the use of hyaluronic acid as a coating system for vesicles could help to develop carriers with biological properties typical of HA, such as regenerative, moisturizing and repairing properties.

2. Materials and Methods

2.1. Materials

The following phospholipids were used for liposome preparation: 1,2-dioleoyl-sn-glycero-3-phosphocholine (DOPC, Sigma, St. Louis, MO, USA) and 1,2-dioleoyl-sn-glycero-3-phosphoethanolamine (DOPE, Sigma, St. Louis, MO, USA). For the coating procedure, hyaluronic acid (HA; Biophil Italia SpA, Origgio, Italy; 8.7 kDa) and chitosan (CH; Sigma, St. Louis, MO, USA; low molecular weight: 50–190 kDa; deacetylation grade, 77%) were used.

The materials were used without any further purification.

2.2. Synthesis of Coated Liposomes

Zwitterionic liposomes were prepared using the thin film hydration method [22] with a main lipid composition of DOPC and DOPE and a final molar ratio of 1:0.5.

2.2.1. CH-Coated Liposomes

In the case of CH-coated liposomes, the lipid compounds were dissolved in chloroform and then dried using a rotary evaporator at 37 °C, which was further dried in a vacuum for 24 h. Subsequently, the dried thin film was hydrated using ultrapure water (pH 7.4; 18.2 MΩ·cm) at 20 °C and then underwent freeze–thaw cycles in liquid nitrogen and a water bath at 50 °C for 9 cycles. The extrusion through 100 nm polycarbonate membranes (27 passages) with LiposoFast apparatus allowed the liposomes to be obtained.

The coating was performed as previously reported in the literature [23]. A freshly prepared CH aqueous solution (4 mg/mL), treated with 0.1% (*v/v*) acetic acid up to a final pH of 4.5, was slowly added drop-by-drop, under magnetic stirring, to the liposome suspension. The coated liposomes were incubated at 4 °C overnight.

2.2.2. HA-Coated Liposomes

The coating of the liposomes with hyaluronic acid (HA) was performed with a solution of low-molecular-weight HA (MW 8.7 kDa; 10 mg/mL) in ultrapure water, type I. The HA solution (1 mL) was used to hydrate the lipidic film during liposome synthesis, before the freeze–thaw and extrusion processes. Then, freeze–thaw cycles in liquid nitrogen and a water bath at 50 °C were performed for 9 cycles, followed by extrusion through a 100 nm

polycarbonate membrane (27 passages) with LiposoFast apparatus, allowed the liposomes to be obtained.

2.3. Purification of Liposomes

The purification of the CH-coated liposomes was obtained by a centrifugation method. Dispersion systems were centrifuged at 4000 rpm for 30 min to remove the excess polymer material. The pellet was then resuspended in distilled water.

The HA-coated liposomes were purified by a dialysis process. The dialysis membrane tubing (cellulose; MW cut-off 14 kDa; ∅ 6 mm) was pre-wetted and washed with several aliquots of ultrapure water to clean the membrane surface. The samples were dialyzed in 50 mL centrifuge tubes in ultrapure water at 4 °C and were shaken every hour. The dialysis water was replaced three times, at regular intervals.

2.4. DLS Analysis

All sizing and ζ-potential measurements were made on a Zetasizer Nano ZS90 (Malvern Instrument Ltd., Malvern, UK) at 25 °C. All measurements were carried out on the liposome samples without any dilution. The Nano ZS incorporates non-invasive backscatter (NIBS™) optics for sizing measurements. The detection angle of 173° enables size measurements of concentrated turbid samples to be performed. However, the scattered light detected from samples during a ζ-potential measurement was made at the forward angle of 12°. All of the measurements were carried out in triplicate, and the results were reported as mean values ± estimated standard deviation (esd).

As the radii of liposomes were always large enough, compared with the Debye–Huckel parameters, the ζ-potentials were calculated directly using the Helmoholtz–Smolowkovski equation (using a Zetasizer) [24]. Sizes were also calculated, using the same experiments, according to the procedure described by Langley [25].

The analyses were performed in triplicate and the results were reported as mean values ± esd.

The significant differences ($p < 0.05$) among data were defined using the one-way analysis of variance (ANOVA) test and the Tukey's test, using Prism 8.0 (GraphPad Software, Inc., San Diego, CA, USA).

2.5. Nuclear Magnetic Resonance (NMR) Experiments

NMR experiments were performed using a Bruker DRX-600 Avance spectrometer operating at 600.13 MHz for 1 h, equipped with an xyz gradient unit. Spectra were processed on Silicon Graphics workstations using Bruker TopSpin software (version 3.6.1).

2.6. ATR-FTIR Analysis

ATR-FTIR spectra were collected via a Nicolet IS50 FTIR spectrophotometer (Thermo Nicolet Corp., Madison, WI, USA) equipped with a single reflection germanium ATR crystal (Pike 16154, Pike Technologies, Fitchburg, WI, USA) and a deuterated triglycine sulphate (DTGS) detector (IR) [26]. Before each experiment, the Ge crystal was cleaned with deionized water and absolute ethanol and dried under a gentle flow of filtered nitrogen. Typically, 32 scans at a resolution of 4 cm^{-1}, in the range of 4000–800 cm^{-1}, were recorded. The frequency scale was internally calibrated with a helium–neon laser reference to an accuracy of 0.01 cm^{-1}. OMNIC software (Version 9.8, Thermo Nicolet) was used for spectra collection and manipulation. The spectrometer was periodically checked by a Nicolet iS50 validation wheel provided by the manufacturer to check the uncertainty, which stood at ±1 cm^{-1} (3059 cm^{-1}; k = 2; 95% confidence level).

The spectral measurements were performed in absorbance mode. To obtain a homogenous and reproducible sample layer over the ATR crystal, the amount of sample (enough to cover the ATR crystal) was dried using a homemade top equipped with a diffusor able to flow dry nitrogen homogeneously onto an ATR crystal surface. Drying took about 5 min at a temperature of 23 ± 2 °C. Three spectral measurements were recorded for each sample

and the averaged spectrum was considered for the study. The sample compartment was normally purged with dry nitrogen but, for these experiments, the flow rate was reduced to the minimum required to obtain a smooth spectrum, whilst avoiding the sample drying.

2.7. Time-of-Flight Secondary Ion Mass Spectrometry (ToF-SIMS) Measurements

ToF-SIMS measurements were carried out on a TRIFT III spectrometer (Physical Electronics, Chanhassen, MN, USA) equipped with a gold liquid metal primary ion source. The liposomes were analyzed as previously described [27,28]. The samples were maintained overnight in the conditioning pre-chamber with a vacuum value of 10^{-5} Pa and then moved to the analyzing chamber, in which the vacuum value was less than 10^{-8} Pa. Positive and negative ion spectra were acquired with a pulsed, bunched 22 keV Au^+ primary ion beam by rastering it over a 100 μm^2 sample area and maintaining static SIMS conditions (primary ion dose density <1012 ions/cm^2). Positive ion spectra were calibrated with CH_3^+ (*m/z* 15.023), $C_2H_3^+$ (*m/z* 27.023) and $C_3H_5^+$ (*m/z* 41.039). The mass resolution (m/Δm) was 3000 at *m/z* 27. Negative ion spectra were not reported because information added to the discussion resulted in these being redundant.

3. Results

3.1. Physicochemical Proprieties of the Coated Liposomes

The liposomes were synthesized as reported in the Experimental Section, and the coating methods were performed to obtain liposomes with a modified surface. In particular, vesicles were coated with one of two different polymers: hyaluronic acid (HA) or chitosan (CH). The goal of this paper was to characterize these liposomes to obtain information about their chemical properties and finally, to optimize the coating procedures.

3.1.1. Size Distribution and ζ-Potential

The results obtained from the physicochemical characterization of the coated and uncoated liposomes are reported in Table 1. The DLS experiments were performed after the purification processes.

Table 1. Size distribution with polydispersity index (PDI) and ζ-potential for all synthesized liposomes. The values are the average of three measurements (mean ± esd) and different letters in the same column indicate significant differences ($p < 0.05$, Tukey's test).

Liposome Composition	Mean Diameter ± esd (nm)	Polydispersity Index (PDI)	ζ-Potential ± esd (mV)
DOPC/DOPE	160.5 ± 3.3 [a]	0.15	25.5 ± 9.4 [a]
DOPC/DOPE-HA	264.4 ± 12.5 [b]	0.20	4.9 ± 3.3 [b]
DOPC/DOPE-CH	450.3 ± 16.7 [c]	0.35	55.3 ± 8.2 [c]

The first step was to analyze the size dimensions of DOPC/DOPE zwitterionic liposomes with any surface modification to understand the behavior of CH and HA during the coating processes. The zwitterionic vesicles showed a hydrodynamic ratio that was in agreement with the extrusion procedure. The dispersions showed average hydrodynamic diameters typically obtained for large unilamellar vesicles, since the values are greater than 100 nm [29]. The PDI values suggested that the liposome solution showed the properties of a pure monodispersing system. The surface charge of 25.5 ± 9.4 mV indicated that such systems are quite stable in solution.

The size of the zwitterionic HA-coated liposomes revealed higher values with respect to the uncoated derivatives (264.4 ± 12.5 nm). These liposomes showed an average diameter that was in perfect agreement with the preparation method, and the PDI value suggested the presence of monodisperse systems. The coating of the liposome with HA deeply modified the surface charge, and the ζ-potential value showed that aggregation/flocculation

processes in solution are very likely. The aggregates can increase their size as a function of storage time.

CH-coated liposomes showed much higher size values with respect to uncoated derivatives (450.3 ± 16.7 nm), with PDI values suggesting a polydisperse system. The ζ-potential value confirmed the strong stability of the suspensions versus time. The values also suggested that the coating process properly occurred, resulting in systems with a higher average diameter than the uncoated liposomes. The coating therefore influences the size of the vesicles, improving their stability and thus preventing aggregation in solution. The higher values obtained could be considered as indicative of excellent stability, since the line between stable and unstable dispersions is generally set at either +30 or −30 mV [30].

DLS experiments highlighted that the liposomes coated with CH had a higher mean diameter than those coated with HA, confirming the presence of CH on the surface of vesicles. The ζ-potential values also confirmed the presence of either of the two polymers on the liposome surfaces.

3.1.2. Nuclear Magnetic Resonance (NMR)

To study the conformational properties of coated liposomes, proton NMR spectra were recorded at 600 MHz and 298 K. In Figure 2, the spectrum of DOPC/DOPE in D_2O is reported. The assignment was carried out as previously reported [31,32] and the typical behavior of the vesicles in solution was revealed: a large signal confirmed the presence of macrosystems in solution and the poor resolution of resonances was a typical characteristic of amphiphilic molecules that form aggregates [33].

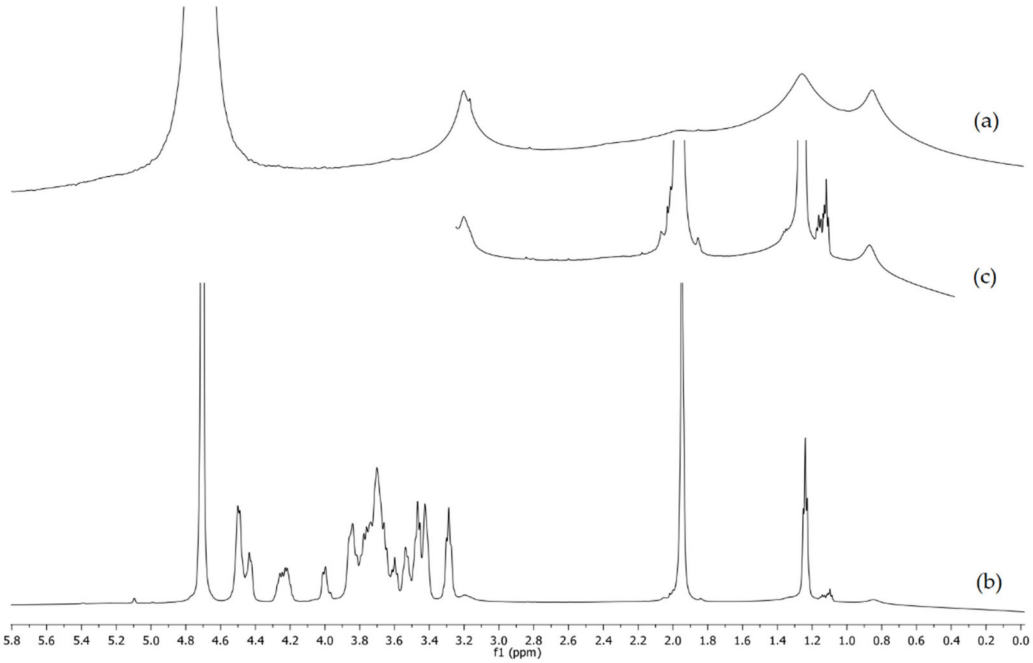

Figure 2. ^{1}H-NMR spectra of: (**a**) DOPC/DOPE uncoated liposomes; (**b**) DOPC/DOPE HA-coated liposomes. (**c**) Magnification of the ^{1}H-NMR spectrum of coated liposomes highlighted the large signal of vesicles in solution.

The NMR spectrum of HA-coated liposomes showed the presence of large signals typical of vesicles (signals at an upfield shift) and the presence of proton signals assigned to HA in solution. In particular, in the range of 3.3–4.5 ppm, NMR signals of the H1–H5 and H1–H6′ protons of glucuronic acid and acetylglucosamine were evident. At 1.98 ppm, the signal of methyl groups of acetylglucosamine were found [34,35]. The chemical shift and the signal width of the HA proton suggest the presence of HA on the liposome surface, which highlights that the coating process occurred properly and that HA was

homogeneously distributed on the liposome surface. The purification process, by means of dialysis, allowed the statement that there was not any free HA in solution.

Figure 3 reports the NMR spectrum of the CH-coated liposome recorded in D_2O at 298 K after the purification processes. In this case, all the NMR signals suggested the presence of large systems in solution. The NMR proton signal at 5.5 ppm was assigned to the H1 of the chitosan, the signal at 3.52 ppm was due to the H3 proton and the H2 signal was at 3.25 ppm. The signal in the range of 3.75–4.34 ppm was assigned to H4, H5, H6 and H6′ protons. The signal at 2.00 ppm was due to the methyl group, -NHCOCH3, of chitin, present in the sample due to the non-total deacetylation of the compound. The large signals at an upfield shift (range 0.5–1.5ppm) were assigned to the DOPC/DOPE liposome [31].

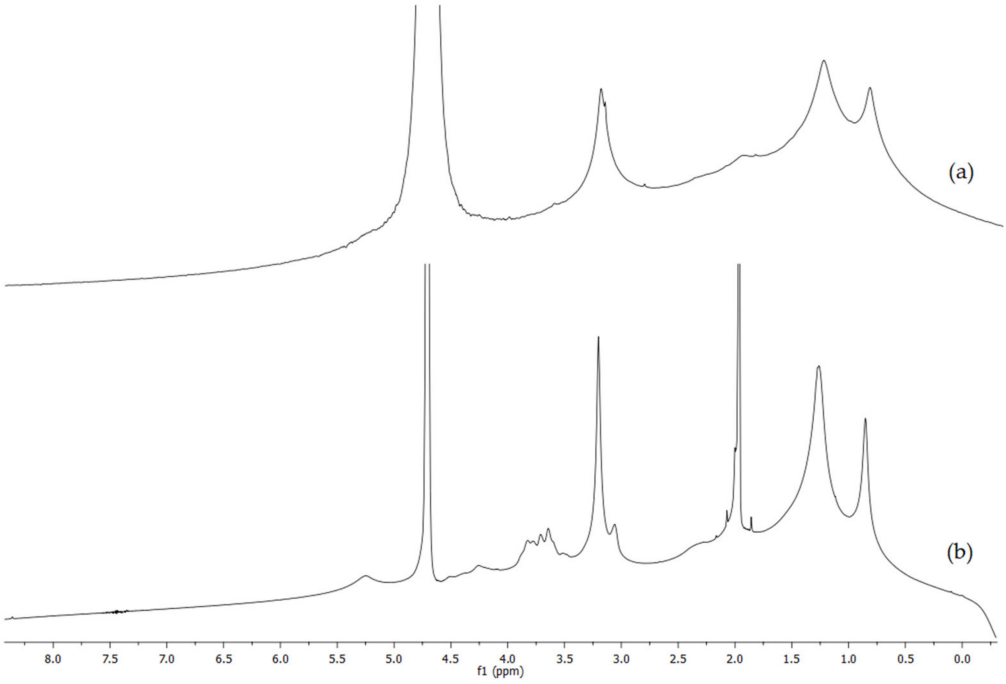

Figure 3. ^{1}H-NMR spectra of: (**a**) DOPC/DOPE liposome; (**b**) DOPC/DOPE coating with CH.

The NMR spectrum confirmed the different sizes obtained for the two different coated liposomes. In particular, the HA-coated DOPC/DOPE systems showed a lower size compared with the CH-coated DOPC/DOPE derivatives. The NMR proton signals of HA and CH suggest the presence of these polymers on the surface of the vesicles.

3.1.3. FTIR-ATR Analysis

Characterization by FTIR-ATR spectroscopy was carried out to examine the influence of a polysaccharide coating on the liposome structure. Figure 4 shows the spectra of a DOPC/DOPE system before and after the coating with the polysaccharides (Figure 4a) and the overlay of the spectra (Figure 4b).

In the 3000–4000 cm^{-1} spectral range, the band at around 3380 cm^{-1} that was formed due to the stretching of the aminic N-H belonging to liposomes, was completely embedded into the broadband due to the strong stretching of the hydroxyl groups and additional NH stretching of the amide groups of the polysaccharides. Symmetric and asymmetric C-H vibrations in the 2850–2855 cm^{-1} range did not show any shift due to the presence of polysaccharide. These wavenumbers have been routinely used to study the phase behavior of lipids because their shift to higher values is attributed to the lipid transition from the gel phase into the liquid–crystalline phase, causing the hydrocarbon chains of the lipids to become more disordered [36]. Regarding the very intense band at 1738 cm^{-1}, attributed to C=O stretching of the lipid ester group, the absence of change in terms of wavenumber and

band shape confirms the very low interaction between the lipids and polysaccharides and, consequently, there is no modification of the hydrogen bonds structures in the interfacial lipid carbonyl groups.

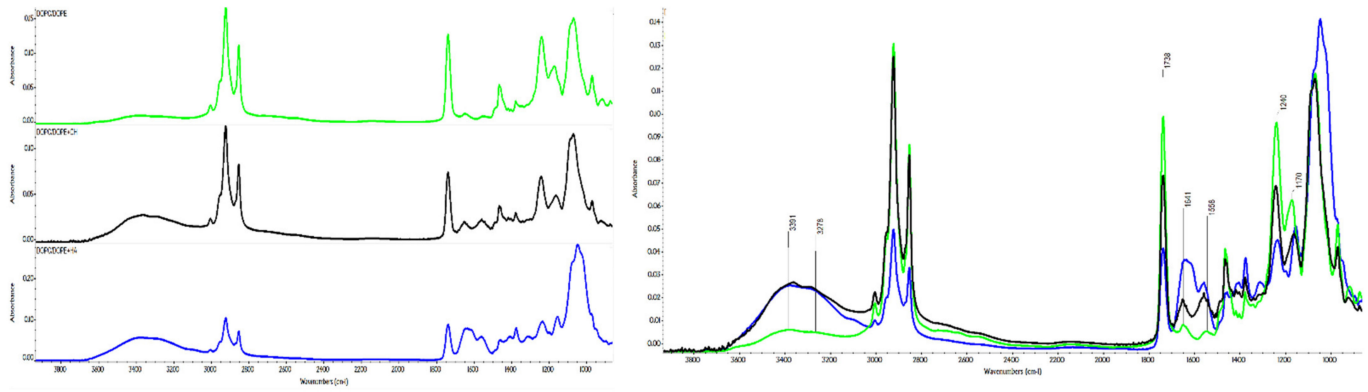

(**a**) (**b**)

Figure 4. ATR-FTIR spectra for (**a**) stacked and (**b**) overlapped DOPC/DOPE (green); DOPC/DOPE-HA (blue); DOPC/DOPE-CH (black) liposomes.

In the range between 1700 and 1500 cm^{-1}, the lipids showed weak bands that were completely embedded in the strong absorption due to the polysaccharide carboxylic/amidic groups.

The intense bands at 1240 cm^{-1} and 1170 cm^{-1} can be attributed to the asymmetric stretching of phosphate diester (PO_2) and the symmetric stretching of ester groups (CO-O-C) in the lipids. The coating by the polysaccharides induces a shift of the ester absorption to 1160 cm^{-1} for the CH coating and to 1158 cm^{-1} for the HA coating. These shifts could be attributed to partial hydrogen bond rearrangement due to the high sensitivity of these vibrations in the hydrogen bond network.

Considering the FTIR analysis as a whole, the presence of polysaccharides is well documented by the bands assigned to amides and saccharides in the 1500–1700 cm^{-1} and 800–1100 cm^{-1} regions, respectively. In addition, the absence of wavenumber shifts and changes in band shape suggests that the polysaccharide coating did not induce major changes in lipid structure.

3.1.4. Time-of-Flight Secondary Ion Mass Spectrometry (ToF-SIMS)

Direct measurement of the lipid composition before and after the coating would add important information. ToF-SIMS analysis was performed with the aim of supporting NMR and IR data. Samples for spectrometric analysis in a vacuum were prepared on a silica surface, which was followed by nitrogen flow drying. To obtain a sensitive and unambiguous measure, all the samples were prepared at the same time with the same amount of compound. The presence of the polysaccharide coating was monitored using reference spectra of bilayers with 1:0.5 DOPC/DOPE, prepared on SiO_2, as was carried out for the other samples. Figures 5 and 6 show the positive ion spectra of DOPC/DOPE coated with chitosan and hyaluronic acid, respectively. In the mass range of *m/z* 150–300, representative for lipids, many fragments were revealed, in particular: the oleate ($C_{18}H_{33}O_2$) peak at *m/z* 281; other characteristic fragments at *m/z* 221 ($C_8H_{15}NO_6^+$) and *m/z* 207 ($C_7H_{13}NO_6^+$); the phospholipidic fragment at *m/z* 184 ($C_5H_{15}NPO_4^+$). After coating the fragments of DOPC/DOPE, the spectrum was very low in intensity and was dominated by the fragment at *m/z* 169, which was not fully characterized but is very common in polysaccharides, including HA and CH. Because of the surface selectivity of ToF-SIMS measurements, these results confirm the presence of a surface coating of polysaccharide.

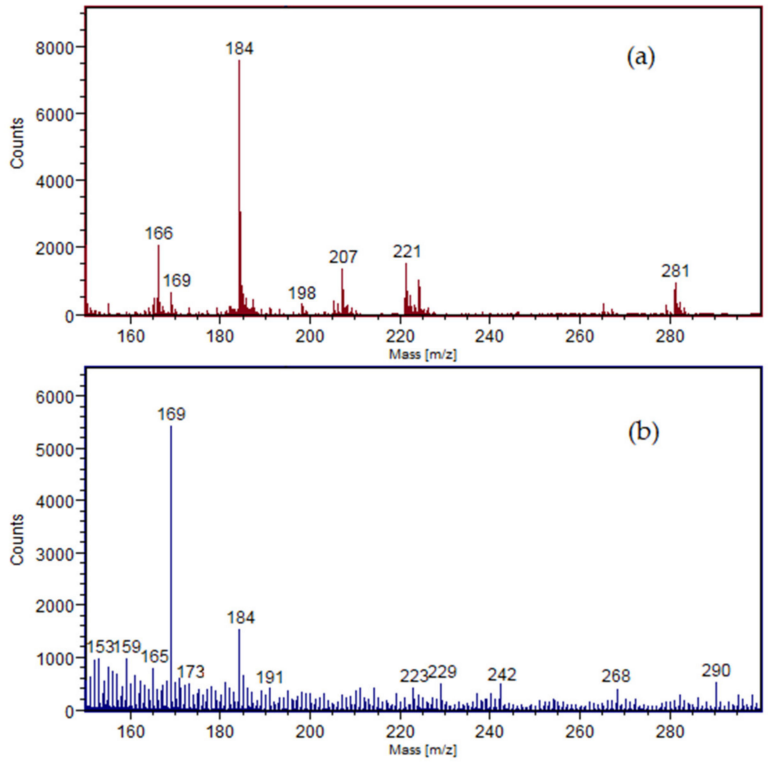

Figure 5. ToF-SIMS positive ion spectra of (**a**) DOPC/DOPE-CH (red); (**b**) CH (blue).

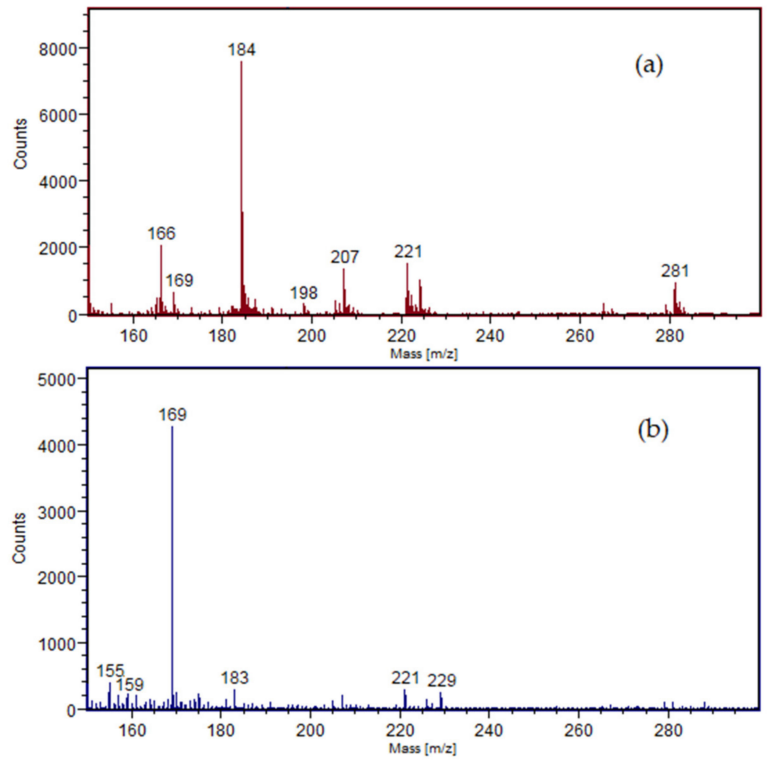

Figure 6. ToF-SIMS positive ion spectra of (**a**) DOPC/DOPE-HA (red); (**b**) HA (blue).

All these experimental data confirm that the coating procedure is correct for zwitterionic liposomes, highlighting that this method is easy and reproducible and allows a very useful drug delivery system to be obtained. Biopolymer-coated liposomes represent a promising and innovative line of research to increase their biological applications and,

in particular, to improve the pharmacological properties of drugs that can be transported to active receptor sites. These systems would be useful to reduce the biodegradability or toxicity problems of encapsulated drugs.

4. Conclusions

The chemical characterization of coated liposomes represents a very important step in the development of new drug delivery systems. In the present work, zwitterionic liposomes coated with two polysaccharides: chitosan and hyaluronic acid, which are widely used for biomedical applications, were synthesized and characterized.

The average size of vesicles being increased after coating with CH and HA, together with the ζ-potential, suggested a proper coating procedure. The ζ-potential of DOPC/DOPE-CH suggested the better physical stability of these preparations, indicating a lower probability of aggregation of liposomes versus time.

The coated liposomes were analyzed by surface infrared (ATR-FTIR) spectroscopy, nuclear magnetic resonance (NMR) and time-of-flight secondary ion mass spectrometry (ToF-SIMS).

The NMR spectra showed the presence of two polymers on the surface of the liposomes. In fact, the proton signals of both liposomes showed broad unresolved peaks, which are typical of aggregates. The comparison of these vesicles suggest that CH coats the vesicles more efficiently.

The analysis of both the infrared and secondary ion mass spectra confirmed the presence of chitosan on the surface of the liposomes. In particular, the ToF-SIMS mass spectra, which investigates the very surface layer of systems (up to a maximum depth of 3–5 nm), provided crucial information on the coating processes.

Author Contributions: Conceptualization, C.B., G.T., A.D. and C.R.; methodology, C.B., G.T., M.C. and A.M.; software, G.L., L.C., V.V. and C.B.; formal analysis, C.B., G.L., M.C. and A.C.; investigation, G.T., M.C. and C.B.; data curation, G.T., C.B. and G.L.; writing—original draft preparation, G.T., M.C., G.L. and C.B.; writing—review and editing, G.T., C.B., G.L., A.C., M.C., L.C., V.V., A.D., C.R. and A.M.; supervision G.T., C.B. and C.R.; project administration, A.M., A.C., A.D. and C.R.; funding acquisition C.R. All authors have read and agreed to the published version of the manuscript.

Funding: This research received no external funding.

Institutional Review Board Statement: Not applicable.

Informed Consent Statement: Not applicable.

Data Availability Statement: Data sharing not applicable.

Conflicts of Interest: The authors declare no conflict of interest.

References

1. Taylor, T.M.; Weiss, J.; Davidson, P.M.; Barry, D.; Bruce, B.D. Liposomal Nanocapsules in Food Science and Agriculture. *Crit. Rev. Food Sci. Nutr.* **2005**, *45*, 587–605. [CrossRef] [PubMed]
2. Son, K.; Ueda, M.; Taguchi, K.; Maruyama, T.; Takeoka, S.; Ito, Y. Evasion of the accelerated blood clearance phenomenon by polysarcosine coating of liposomes. *J. Control. Release* **2020**, *322*, 209–216. [CrossRef] [PubMed]
3. Knop, K.; Hoogenboom, R.; Fischer, D.; Schubert, U.S. Poly(ethylene glycol) in drug delivery: Pros and cons as well as potential alternatives. *Angew. Chem. Int. Ed.* **2010**, *49*, 6288–6308. [CrossRef] [PubMed]
4. Elbassiouny, S.; Fadel, M.; Elwakil, T.; Elbasiouny, M.S. Photodynamic diagnosis of parathyroid glands with nano-stealth aminolevulinic acid liposomes. *Photodiagnosis Photodyn. Ther.* **2018**, *21*, 71–78. [CrossRef]
5. Kushwah, V.; Jain, D.K.; Agrawal, A.K.; Jain, S. Improved antitumor efficacy and reduced toxicity of docetaxel using anacardic acid functionalized stealth liposomes. *Colloids Surf. B Biointerfaces* **2018**, *172*, 213–223. [CrossRef]
6. Xi, L.; Li, C.; Wang, Y.; Gong, Y.; Su, F.; Li, S. Novel Thermosensitive Polymer-Modified Liposomes as Nano-Carrier of Hydrophobic Antitumor Drugs. *J. Pharm. Sci.* **2020**, *109*, 2544–2552. [CrossRef]
7. Ramezanzade, L.; Hosseini, S.F.; Adergani, B.A.; Yaghmur, A. Cross-linked chitosan-coated liposomes for encapsulation of fish-derived peptide. *LWT-Food Sci. Technol.* **2021**, *150*, 112057–112065. [CrossRef]

8. Hermal, F.; Frisch, B.; Specht, A.; Bourel-Bonnet, L.; Heurtault, B. Development and characterization of layer-by-layer coated liposomes withpoly(L-lysine) and poly(L-glutamic acid) to increase their resistance in biological media. *Int. J. Pharm.* **2020**, *586*, 119568–119579. [CrossRef] [PubMed]
9. Patra, J.K.; Das, G.; Fraceto, L.F.; Ramos Campos, E.V.; Rodriguez-Torres, M.; Acosta-Torres, L.S.; Diaz-Torres, L.A.; Grillo, R.; Swamy, M.K.; Sharma, S.; et al. Nano based drug delivery systems: Recent developments and future prospects. *J. Nanobiotechnol.* **2018**, *16*, 71–104. [CrossRef] [PubMed]
10. Din, F.; Aman, W.; Ullah, I.; Qureshi, O.S.; Mustapha, O.; Shafique, S.; Alam Zeb, A. Effective use of nanocarriers as drug delivery systems for the treatment of selected tumors. *Int. J. Nanomed.* **2017**, *12*, 7291–7309. [CrossRef]
11. Lane, R.-S.; Haller, F.M.; Chavaroche, A.A.E.; Almond, A.; DeAngelis, P.L. Heparosan-coated liposomes for drug delivery. *Glycobiology* **2017**, *27*, 1062–1074. [CrossRef]
12. Rojas Ramirez, R.E.; Souza Orth, E.; Pires, C.; Zawadzki, S.F.; Alves de Freitas, R. DODAB-DOPE liposome surface coating using in-situ acrylic acid polymerization. *J. Mol. Liq.* **2021**, *330*, 115689. [CrossRef]
13. Volodkin, D.; Mohwald, H.; Voegel, J.C.; Ball, V. Coating of negatively charged liposomes by polylysine: Drug release study. *J. Control. Release* **2007**, *117*, 111–120. [CrossRef] [PubMed]
14. Gonzalez Rodriguez, M.L.; Barros, L.B.; Palma, J.; Gonzalez Rodriguez, P.L.; Rabasco, A.M. Application of statistical experimental design to study the formulation variables influencing the coating process of lidocaine liposomes. *Int. J. Pharm.* **2007**, *337*, 336–345. [CrossRef] [PubMed]
15. Chaves, M.A.; Pinho, S.C. Curcumin-loaded proliposomes produced by the coating of micronized sucrose: Influence of the type of phospholipid on the physicochemical characteristics of powders and on the liposomes obtained by hydration. *Food Chem.* **2019**, *291*, 7–15. [CrossRef] [PubMed]
16. Bonechi, C.; Lamponi, S.; Donati, A.; Tamasi, G.; Consumi, M.; Leone, G.; Rossi, C.; Magnani, A. Effect of resveratrol on platelet aggregation by fibrinogen protection. *Biophys. Chem.* **2017**, *222*, 41–48. [CrossRef]
17. Liu, M.; Zhang, Y.; Wu, C.; Xiong, S.; Zhou, C. Chitosan/halloysite nanotubes bionanocomposites: Structure, mechanical properties and biocompatibility. *Int. J. Biol. Macromol.* **2012**, *51*, 566–575. [CrossRef]
18. Huynh, A.; Priefer, R. Hyaluronic acid applications in ophthalmology, rheumatology, and dermatology. *Carbohydr. Res.* **2020**, *489*, 107950–107956. [CrossRef]
19. Li, Y.; Ruan, S.; Wang, Z.; Feng, N.; Zhang, Y. Hyaluronic Acid Coating Reduces the Leakage of Melittin Encapsulated in Liposomes and Increases Targeted Delivery to Melanoma Cells. *Pharmaceutics* **2021**, *13*, 1235. [CrossRef] [PubMed]
20. Wan, W.J.; Huang, G.; Wang, Y.; Tang, Y.; Li, H.; Jia, C.H.; Liu, Y.; You, B.G.; Zhang, X.N. Coadministration of iRGD peptide with ROS-sensitive nanoparticles co-delivering siFGL1 and siPD-L1 enhanced tumor immunotherapy. *Acta Biomater.* **2021**, *136*, 473–484. [CrossRef] [PubMed]
21. Fukushige, K.; Tagami, T.; Naito, M.; Goto, E.; Hirai, S.; Hatayama, N.; Yokota, H.; Yasui, T.; Baba, Y.; Ozeki, T. Developing spray-freeze-dried particles containing a hyaluronic acid-coated liposome-protamine-DNA complex for pulmonary inhalation. *Int. J. Pharm.* **2020**, *583*, 119338–119345. [CrossRef] [PubMed]
22. Zhao, Z.; Zhao, Y.; Xie, C.; Chen, C.; Lin, D.; Wang, S.; Lin, D.; Cui, X.; Guo, Z.; Zhou, J. Dual-active targeting liposomes drug delivery system for bone metastatic breast cancer: Synthesis and biological evaluation. *Chem. Phys. Lipids* **2019**, *223*, 104785. [CrossRef] [PubMed]
23. Jøraholmen, M.W.; Škalko-Basnet, N.; Acharya, G.; Basnet, P. Resveratrol-loaded liposomes for topical treatment of the vaginal inflammation and infections. *Eur. J. Pharm. Sci.* **2015**, *79*, 112–121. [CrossRef] [PubMed]
24. Hunter, R.J. *Zeta Potential in Colloid Science: Principles and Application*, 1st ed.; Academic Press: London, UK, 1988.
25. Langley, K.H. Developments in electrophoretic laser light scattering and some of biochemical applications. In *Laser Light Scattering in Biochemistry*; Harding, S.E., Sattelle, D.B., Bloomfield, V.A., Eds.; The Royal Society of Chemistry: Cambridge, UK, 1992; pp. 151–160.
26. Leone, G.; Consumi, M.; Pepi, S.; Lamponi, S.; Bonechi, C.; Tamasi, G.; Donati, A.; Rossi, C.; Magnani, A. Alginate–Gelatin Formulation to Modify Lovastatin Release Profile from Red Yeast Rice for Hypercholesterolemia Therapy. *Ther. Deliv.* **2017**, *8*, 843–854. [CrossRef] [PubMed]
27. Leone, G.; Consumi, M.; Lamponi, S.; Bonechi, C.; Tamasi, G.; Donati, A.; Rossi, C.; Magnani, A. Hybrid PVA-Xanthan Gum Hydrogels as Nucleus Pulposus Substitutes. *Int. J. Polym. Mat.* **2019**, *68*, 681–690. [CrossRef]
28. Leone, G.; Consumi, M.; Lamponi, S.; Bonechi, C.; Tamasi, G.; Donati, A.; Rossi, C.; Magnani, A. Thixotropic PVA hydrogel enclosing a hydrophilic PVP core as nucleus pulposus substitute. *Mater. Sci. Eng. C* **2019**, *98*, 696–704. [CrossRef] [PubMed]
29. Pinheiro, L.; Reis, L. Liposomes as drug delivery systems for the treatment of TB. *Nanomedicine* **2011**, *6*, 1413–1428. [CrossRef] [PubMed]
30. Greenwood, R.; Kendall, K. Selection of suitable dispersants for aqueous suspensions of zirconia and titania powders using Acoustophoresis. *J. Eur. Ceram. Soc.* **1999**, *19*, 478–488. [CrossRef]
31. Bonechi, C.; Ristori, S.; Martini, G.; Martini, S.; Rossi, C. Study of bradykinin conformation in the presence of model membrane by Nuclear Magnetic Resonance and molecular modelling. *Biochim. Biophys. Acta* **2009**, *1788*, 708–716. [CrossRef] [PubMed]
32. Bonechi, C.; Ristori, S.; Martini, S.; Panza, L.; Martini, G.; Rossi, C.; Donati, A. Solution behavior of a sugar-based carborane for boron neutron capture therapy: A nuclear magnetic resonance investigation. *Biophys. Chem.* **2007**, *125*, 320–327. [CrossRef] [PubMed]

33. Ramanathan, M.; Shrestha, L.K.; Mori, T.; Ji, Q.; Hill, J.P.; Ariga, K. Amphiphile nanoarchitectonics: From basic physical chemistry to advanced applications. *Phys. Chem. Chem. Phys.* **2013**, *15*, 10580–10611. [CrossRef] [PubMed]
34. Mendes, M.; Cova, T.; Basso, J.; Ramos, M.L.; Vitorino, R.; Sousa, J.; Pais, A.; Vitorino, C. Hierarchical design of hyaluronic acid-peptide constructs for glioblastoma targeting: Combining insights from NMR and molecular dynamics simulations. *J. Mol. Liq.* **2020**, *315*, 113774. [CrossRef]
35. Donati, A.; Magnani, A.; Bonechi, C.; Barbucci, R.; Rossi, C. Solution structure of hyaluronic acid oligomers by experimental and theoretical NMR, and molecular dynamics simulation. *Biopolymers* **2001**, *59*, 434–445. [CrossRef]
36. Tuchtenhagen, J.; Ziegler, W.; Blume, A. Acyl Chain conformational ordering in liquid-crystalline bilayers: Comparative FT-IR and 2H-NMR studies of phospholipids differing in headgroup structure and chain length. *Eur. Biophys. J.* **1994**, *23*, 323–335. [CrossRef]